PERMAFROST - Seventh International Conference (Proceedings),
Yellowknife (Canada), Collection Nordicana No 55, 1998

SEASONAL STRUCTURE OF TALIKS BENEATH ARCTIC STREAMS DETERMINED WITH GROUND-PENETRATING RADAR

Steven A. Arcone, Edward F. Chacho, Allan J. Delaney

U. S. Army Cold Regions Research and Engineering Laboratory, 72 Lyme Road, Hanover, NH 03755

Abstract

We interpret the structure and development of taliks beneath stream channels from 375-MHz ground-penetrating radar profiles obtained in January and April within the Sagavanirktok River floodplain in Alaska. The upper surfaces appear smooth, often show an ice layer, and vary in depth with channel bathymetry. Partial freezing within taliks appears to cause weak reflections from the talik surface, internal reflections, and a distorted talik radar image. The taliks shrink as they propagate downward through the winter. Some taliks completely freeze by mid-April. Others may exist at 3.7 m beneath a typical, 1.8-m-deep frozen channel, and deeper beneath channels that do not freeze completely. The persistent though diminishing flow from drill holes demonstrates their permeability.

Introduction

Permafrost underlies the flood plains of Alaska's North Slope. Within the permafrost, taliks (or "thaw bulbs") reside beneath many arctic river channels. Extensive taliks (Wankiewicz, 1984) could provide a significant water source in winter, and a means of contaminant transport from developed areas to the ocean. They are also a possible source of surface icing (Carey, 1973). Cross sectional definition of taliks by drilling is time consuming and costly. In this paper we interpret the cross-sectional structure of some taliks beneath channels of the Sagavanirktok River from ground-penetrating radar (GPR) profiles. We use boreholes and existing information to derive material dielectric permittivities to aid interpretation. We obtained the profiles in January and April 1992 and in April 1993 to look at seasonal development. We previously used GPR on the Sagavanirktok flood plain to profile water beneath ice mounds (Arcone et al., 1990; Chacho et al., 1991) and stream channels (Arcone et al., 1992).

Equipment and methods

We used the GSSI (Geophysical Survey Systems, Inc.) models 4800 radar control unit, DT6000 digital tape drive, and 3102 antenna transducer. The antennas were polarized perpendicular to the transect direction and dragged behind a Hagglunds B111 vehicle (Figure 1) at about 2 m/s. The GPR wavelet (Figure 1) lasted about 2.5 cycles and its bandwidth was centered near 375 MHz. Most of the radiation was centered about a 60° cone (Arcone, 1995). We used a Garmin GPS navigator to set our transects (30 m estimated accuracy). April 1992 transects generally retraced the visible vehicle tracks from January. Profile distance in 1992 was not metered because of the length of the lines, but segment lengths are well estimated from the constant vehicle speed and rate of data acquisition. Profile distance in April 1993 was measured at drill locations.

We recorded at 25.6 traces/s, a density of 512 8-bit samples/trace, and used a time-dependent gain to compensate loss in signal amplitude caused by wavefront spreading. We used band pass trace filtering to reduce electronic and antenna-ground coupling noise, spatial filtering to alleviate antenna direct coupling and multiple reflections, and in some cases, Kirchhoff time migration, despite the variable permittivity, to reduce diffractions and better position horizons (Yilmaz, 1987). We determined dielectric permittivity contrasts across reflecting interfaces from the sign of the interface reflection coefficient, which we determined from the

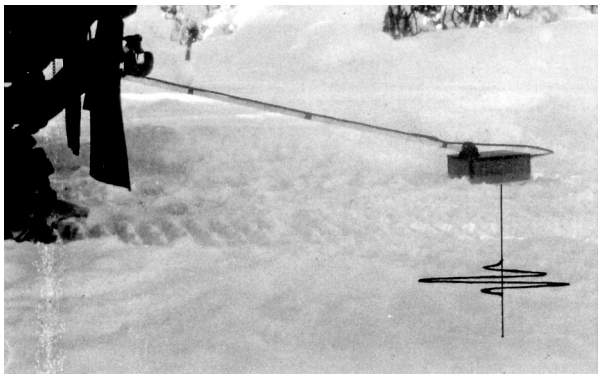

Figure 1. Transmitter and receiver antenna transducer towed behind a Hagglunds B111 vehicle. The transmitted waveform is represented.

Figure 2. Drill rig with water spouting from a talik.

sequences of phase polarities for the half-cycles of the reflected wavelets (Arcone et al., 1998). A gray scale profile format indicates positive phase with light tones and negative with dark. Phase for the same reflections are opposite between years because we used differently wired transducers.

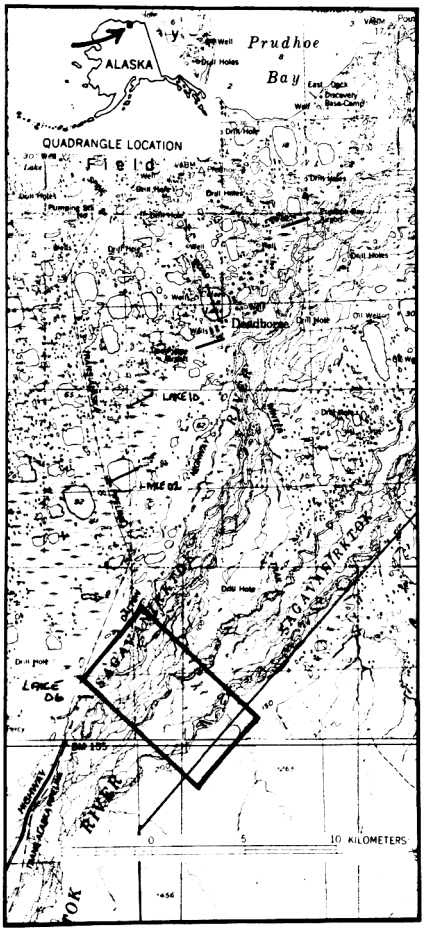

Figure 3. Survey area on the Sagavanirktok River floodplain.

We interpreted layer thickness, d (cm), with the geometric optics formula, $d = ct/2\varepsilon^{1/2}$, where c is the speed of light (30 cm/ns), t is the round trip time delay between the layer reflections, and ε is the real part of the material dielectric permittivity. The time reference (i.e., the ground surface) is the time of transmission. The ε of ice and water are 3.2 and 88 (predominantly real at 0°C), respectively, within our bandwidth. An assumed water conductivity of less than 0.02 Siemens/m does not affect ε of wet sediments at our frequency. The ε of frozen sands and gravels at low ice contents is about 5 (Arcone et al., 1992; 1998), but is recalculated here for areas of suspected high ice content.

We estimate a value of ε = 30 for the unfrozen sands and gravels of a talik. Although laboratory measurements of Topp et al. (1980) range from 15-20 for saturated sandy soils at a volumetric water contents of about 25%, Alaskan field measurements at the same water content, but near 0°C range from 25–40 for nearly pure sands (Arcone et al., 1998). The lower laboratory values are caused by the lower ε of water at 20°C, and by water adsorption on the larger silt and clay fractions (Hoekstra and Delaney, 1974; Topp et al., 1980). We place our ε nearer the low end of the field values because of the small gravel content observed in the drilling. An error in ε of as much as 20% would cause only a 10% error in d because of the square root dependency.

We recorded snow, ice and talik depths, and noted sediment type during drilling. The pressurized water (Figure 2) encountered when a talik was penetrated prevented further drilling.

Results and discussion

The study area is between the Dalton Highway and Franklin Bluffs at about 25 km from Prudhoe Bay (Figure 3). Gravel bars, and icings give minor relief to the flood plain here. Snow thickness generally ranged between 5 and 25 cm. The profiles were generally across the stream directions. We cannot identify any particular stream from the outdated topographic quadrangle maps. We do not discuss profiles obtained over deep channels that had not completely frozen because our time range prevented recording of reflections from the bottom of the taliks.

Control Lines

We obtained these profiles (Figure 4) in April 1993, along with drilling to verify the presence of free water and to obtain talik depths in order to determine ε for the cyclically frozen ground above them. The reflections from the bottom of the channel ice and from the top surface of the talik have the same phase (tone sequence

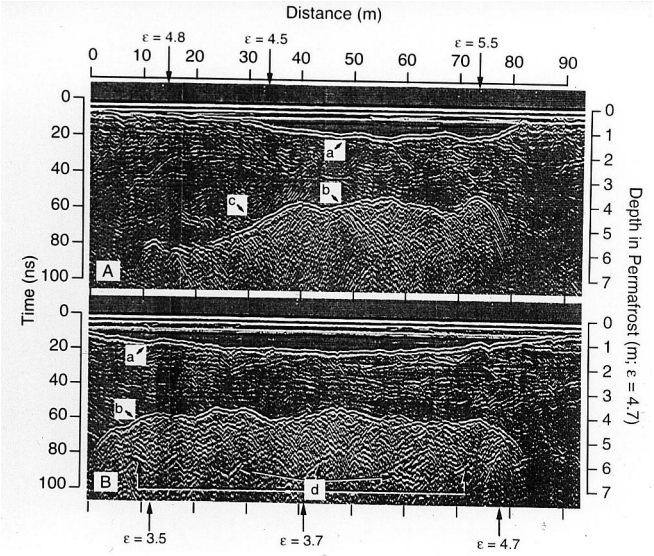

Figure 4. Profiles along two sections of the control line. Vertical arrows locate boreholes where we calculated ε for the frozen alluvium above the talik. Labeled events are bottom of channel ice (a), talik surface (b), ice layer (c), bottom of talik (d). The direct coupling between antennas at 0 ns is the surface reference. The maximum ice thickness is 1.5 m in the top profile and 1.7 m in the bottom.

in their reflection bands) and are, therefore, from interfaces between materials of lower ε above, and of higher ε below. Intermittent reflections from the bottom of the talik are evident only in profile B. The hyperbolically shaped diffractions from within the taliks indicate an inhomogeneous permittivity structure. Weak reflections and diffractions throughout the frozen material indicate slight variations in its permittivity.

The drilling depths and reflection times give an ε between 4.5 and 5.5 near the ends of the taliks or where they are deeper. These values are typical for alluvial permafrost (Arcone and Delaney, 1989; Arcone et al., 1992) and represent an ice content of probably less than 20%. The lower values above the main part of the taliks in profile B indicate an ice content in excess of 70% (Delaney and Arcone, 1984; Arcone and Delaney, 1989). We interpret a decrease in drilling resistance encountered just before free water was reached at 33 m distance in profile A to indicate an ice layer, whose reflection is marked in the profile. The free water from the talik rose approximately 60 cm above the ground surface and then settled to a slow trickle that lasted over 30 minutes.

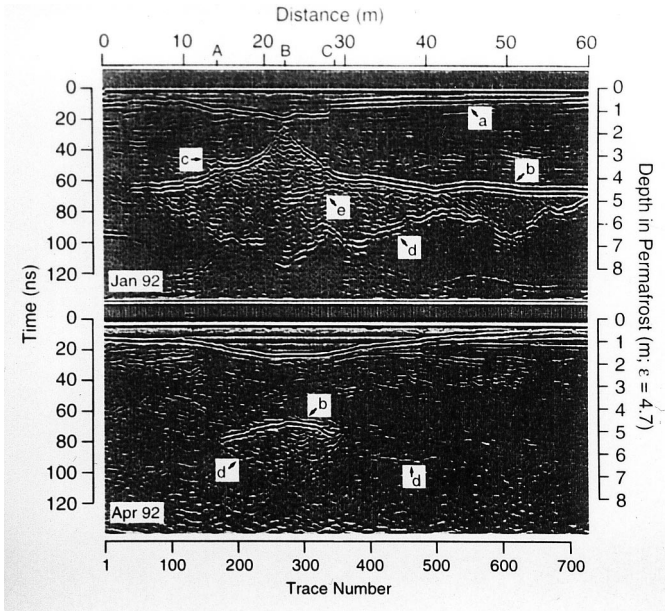

Figure 5. Time-migrated seasonal profiles of a talik. Profile events are labeled as in Figure 4. We interpret the area within the talik above event (e) to be partially frozen. The maximum channel ice thickness is about 1.6 m.

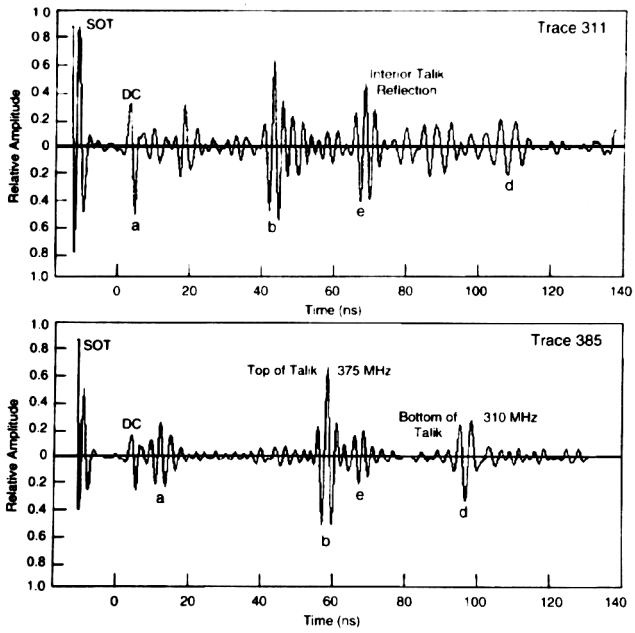

Figure 6. Sample traces, with the same letter labels, from Figure 5. Added gain makes the waveforms more visible. SOT (start-of-trace) is an artificial signal that triggers recording. DC, the direct coupling (partially filtered) between antennas, represents the channel ice surface. The reflections from the top and bottom of the talik have different phases. Trace 311, at 25 m distance, shows the strong reflection from within the talik. The phase agreement for the ice bottom, talik surface and internal talik reflections indicates increasing values of ε across each interface. The shift in local wavelet frequency to about 310 MHz (trace 385, at 30 m distance), is characteristic of propagation in a wet medium.

Partial Freezing of a Talik, and Ice Layers

We compare cross-sectional profiles of a talik in January and April 1992 in Figure 5. In January the talik was thickest beneath the deepest part of the channel, where it had just lost contact with the ice bottom. Only a small talik remained in April and a lower surface is barely discernible. The difference in phase between the talik top and bottom reflections (trace 385 in Figure 6) verifies the expected contrasts in ε across the interfaces. We interpret the reflection between points A and C within the January talik to be from the bottom of a partially frozen zone that extends to the talik surface. The relative strength of this reflection is seen in trace 311 of Figure 6. Partial freezing is also consistent with the generally weaker strength of the talik surface reflection near point B where only 1.5 cycles are visible in the profile. The greater signal strength outside of points A and

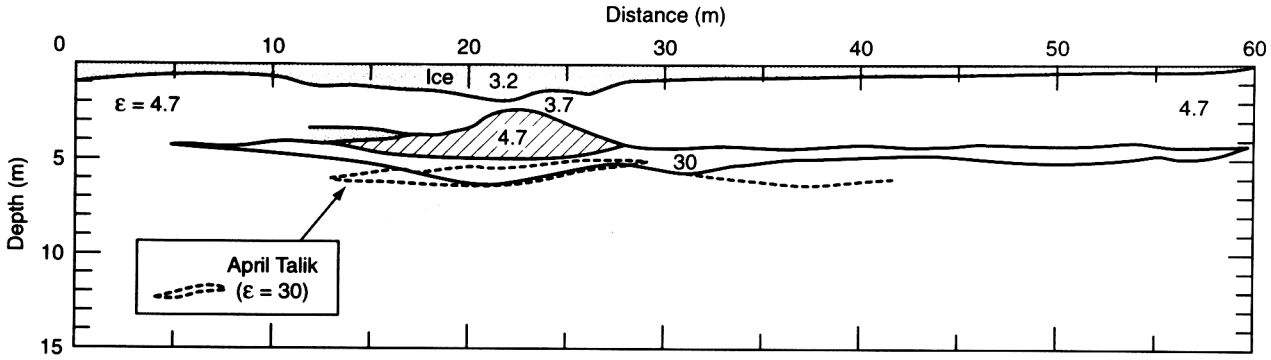

Figure 7. Interpretations of the profiles in Figure 5. Permittivity values for each section are labeled. The cross hatched area is a partially frozen section of the January talik. The talik appears to have migrated deeper by April.

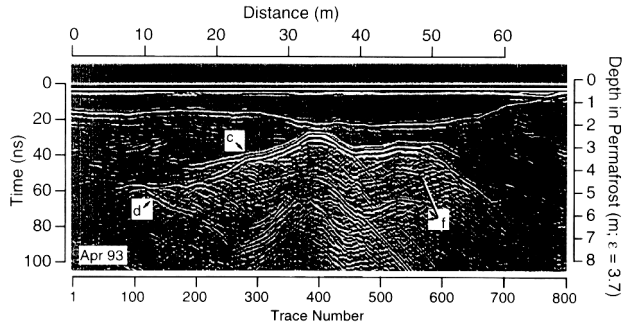

Figure 8. Profile of a talik recorded in April 1993. We interpret the reflections above the entire talik surface to be from a layer of ice. Events (f) are multiple reflections between the talik surface and the top and bottom surfaces of the channel ice.

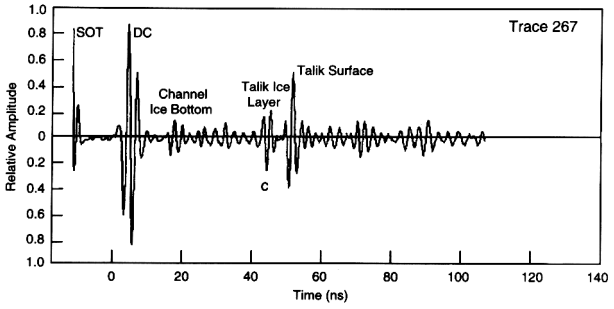

Figure 9. Trace 267 from the profile in Figure 8. The phase opposition between the reflections from the talik ice layer and talik surface is consistent with the sequences of higher e (frozen sediments) over lower e (ice) vs., lower e (ice) over higher e (unfrozen or partially frozen sediments), respectively.

C, which makes all 2.5 cycles visible, is consistent with a completely unfrozen state. As seen in the previous example, there is evidence of an accretionary ice layer (event c in the profile) on the surface of the talik.

We present our values of ε and interpret the talik structures in Figure 7. We interpolated the control line calculations for the frozen sediments surrounding the upper surface of the talik in January to give ε values which linearly decreased from 4.7 at less than 2-m and greater than 40-m distances, to 3.7 near the center at 22 m. The 3.7 value corresponds with a volumetric ice content of about 73% (Delaney and Arcone, 1984). If this percentage held throughout the talik, we find that only about 1% of the remaining volume within the upper portion of the talik between points A and C needs to have been unfrozen water to have provided an ε = 4.7

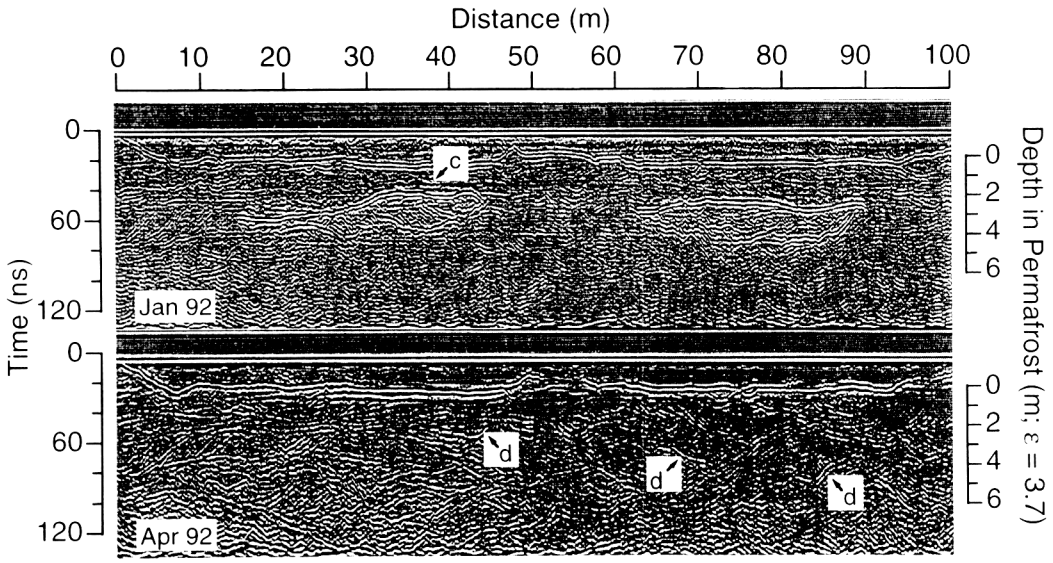

Figure 10. Time-migrated profiles of two taliks recorded in mid-January and mid-April 1992. Events (d) are interpreted as remnants of the lower surface of the taliks. An ice layer (event c) may exist over the left side talik.

(using the refractive index mixing model - Annan et al., 1994) and have generated the observed weak reflections with the proper phase. Most of the talik that is interpreted to have been totally melted in January appears to have been less than 1 m thick and with a bottom surface of fairly uniform depth. We interpret this bottom surface to have moved about 1.3 m deeper by April. It is also possible that the April talik was partially frozen.

Evidence of a more extensive ice layer along the surface of another talik is seen in Figure 8. The maximum channel ice thickness was 2.0 m. The bottom of this channel had probably remained unfrozen throughout most of the winter because the talik is close to the ice bottom. The maximum thickness of the talik ice layer was about 1.2 m. The interpretation is consistent with the relative phases of the reflections (Figure 9).

Complete Freezing of a Talik

We profiled two closed taliks that froze completely by mid-April (Figure 10). The maximum channel ice thickness above both taliks was 2.0 m. Several short horizons in April (events d) appear to have been part of the lower surface of the January taliks because they have similar configurations. Given $\varepsilon = 3.7$ for ice-rich sediments at about the 65-m distance, the top of the talik in January was 2.0 m deep and the remnant bottom horizon in the April profile was 3.7 m deep. If the January talik's bottom depth at this distance was 2.4 m, then the 15-ns delay within the 0.4-m-thick talik at this point gives a reasonable $\varepsilon = 32$ (totally unfrozen). We then estimate the total downward movement to have been 1.3 m from mid-January to mid-April, which is similar to the displacement interpreted for the previous example.

Conclusions

By mid-winter, many taliks appear to be a thin layer which extends over nearly the width of the channel. Although taliks beneath channels less than about 1.8 m deep appear to be gone by winter's end, taliks profiled in April beneath thicker and completely frozen streams may have obtained their heat from a thicker part of the talik that was not profiled. The continuous reflections from the talik surfaces imply that freezing fronts were smooth to within a few centimeters. Partial melt within a talik may be attributed to adsorbed water on the small fractions of silt and clay particles. Variations in ε and in situ wavelengths of 15–18 cm within unfrozen parts of the taliks explain the many diffractions and the radar sensitivity to internal talik structure. The continuous flow from the drill holes demonstrates permeability, and the pressurized condition shows that talik water is probably slightly below 0°C. Large taliks can provide a significant water source in late winter, and radar is an ideal tool for their location.

Acknowledgments

This research was funded by the U.S. Army corps of Engineers RDTE long range program research in snow, ice and frozen ground, Project 4A161102AT24.

References

Annan, A.P., Cosway, S.F. and Sigurdsson, T. (1994). GPR for snowpack water content. In Redman, J.D. and Watson, E.M. (eds.), Proceedings of the 5th International Conference on Ground-Penetrating Radar, Waterloo, Ontario, University of Waterloo, pp. 465–475.

Arcone, S.A. (1995). Numerical studies of the radiation patterns of resistively loaded dipoles. *Journal of Applied Geophysics*, 33, 39–52.

Arcone, S.A., Chacho, E.F., Jr. and Delaney, A.J. (1990). Ice mounds on the Sagavanirktok River. In Murthy, T.K.S. (ed.), Ice Technology for Polar Operations: Proceedings of the Second International Conference on Ice Technology, Cambridge, U.K. Computational Mechanics Publications: Southampton, Boston, pp. 353–363.

Arcone, S.A., Chacho, E.F., Jr. and Delaney, A.J. (1992). Short-pulse radar detection of groundwater in the Sagavanirktok flood plain in early spring. *Water Resources Research*, 28, 2925–2936.

Arcone, S.A. and Delaney, A.J. (1989). Investigations of dielectric properties of some frozen materials using cross-borehole radiowave pulse transmission. CRREL Report 89-4, U.S. Army Cold Regions Research and Engineering Laboratory, Hanover, NH, 18 pp.

Arcone, S.A., Lawson, D.E., Delaney, A.J., Strasser, J.C. and Strasser, J.D. (1998). Ground-penetrating radar reflection profiling of groundwater and bedrock in an area of discontinuous permafrost. *Geophysics*, in press.

Carey, K.L. (1973). Icings developed from surface water and ground water. Monograph III-D3, U.S. Army Cold Regions Research and Engineering Laboratory, Hanover, NH, 18 pp.

Chacho, E.F., Jr., Collins, C.M., Delaney, A.J. and Arcone, S.A. (1991). River icing mounds: A winter water source on the eastern north slope of Alaska. In Prowse, T.D. and Ommaney, C.S.L. (eds.), Northern Hydrology: Selected Perspectives: Proceedings of the Northern Hydrology Symposium 10–12 July 1990, Saskatoon, Saskatchewan, National Hydrology Research Institute Symposium No. 6: Saskatoon SA, pp. 33-45.

Delaney, A.J. and Arcone, S.A. (1984). Dielectric measurements of frozen silt using time domain reflectometry. *Cold Regions Science and Technology*, 9, 39–46.

Hoekstra, P. and Delaney, A.J. (1974). Dielectric properties of soils at UHF and microwave frequencies. *Journal of Geophysical Research*, 79, 1699–1708.

Topp, G.C., Davis, J.L. and Annan, A.P. (1980). Electromagnetic determination of soil water content: measurements in coaxial transmission lines. *Water Resources Research*, 16, 574–582.

Wankiewicz, A. (1984). Hydrothermal processes beneath arctic river channels. *Water Resources Research*, 20, 1417–1426.

Yilmaz, O. (1987). Seismic data processing. Society of Exploration Geophysicists: Tulsa, OK.